Localization and Orientation of Homopolymer in Block Copolymer Lamella: A Near-Field Optical Microscopy Study

Jian Yang, Ryojun Sekine, Hiroyuki Aoki,* and Shinzaburo Ito

Department of Polymer Chemistry, Graduate School of Engineering, Kyoto University, Katsura, Kyoto 615-8510, Japan

Received June 18, 2007; Revised Manuscript Received August 8, 2007

ABSTRACT: The experiments described here were designed to characterize the location and orientation of a single homopolymer chain embedded in a block copolymer lamella. We used scanning near-field optical microscopy (SNOM) to image individual perylene-labeled poly(methyl methacrylate) (PMMA-Pe) chains sparsely distributed in lamellar phases formed by poly(styrene-*b*-methyl methacrylate) (PS−PMMA). By calculating the center of mass (CM) of the PMMA-Pe chain, we found that the homopolymer chains were distributed throughout the PMMA-rich domain layers, with the maximum CM population at the domain centers. The orientation of the homopolymer chains is dependent on the location of the CM of the homopolymer in the PMMA block domain. If the CM locates at the domain center, the homopolymer chain prefers an orientation parallel with the lamella. If the CM is close to the block interface, the homopolymer chain tends to orient itself perpendicularly to the interface. This location dependence of chain orientation is likely the result of the rotational freedom of PMMA-Pe chains in the PMMA-rich domains of the PS−PMMA block copolymer lamella.

Introduction

Melts of block copolymers undergo disorder−order transition when the product of the Flory−Huggins interaction parameter (χ_{FH}) and the degree of polymerization (N) exceeds 10.6.[1] Confined by the covalent bond between blocks, block copolymers can only phase-separate on the microscopic scale and self-assemble into various ordered structures such as spheres, cylinders, and lamellae.[2] The scale of block copolymer self-assembly is directly related to the sizes of the blocks. Therefore, the periodicity of self-assembled patterns formed by block copolymers is normally in the 10−100 nm range.

In recent years, there has been strong interest in studying homopolymer blends with block copolymers. When a homopolymer A dissolves in a matrix of a block copolymer A-*b*-B, where the two constituent polymers A and B are immiscible, the homopolymer will be confined to the A-rich domain formed by the block copolymer. This confinement results in entropy loss of the system. As an energetic compensation, individual homopolymers may have preferred locations, conformations, and orientations in the block domains.

Studies of homopolymer localization in block copolymer lamellae have been widely explored both theoretically[3,4] and experimentally by small-angle X-ray and neutron scattering,[5] transmission electron microscopy,[6] atomic force microscopy,[7] specular neutron reflectivity,[8,9] and fluorescence resonance energy transfer.[10] If the concentration of the homopolymer is low enough, the presence of the homopolymer will not alter the lamellar structure of the block copolymer. The location of the homopolymer in the block copolymer lamella mainly depends on the molecular weights of the homopolymer A (M_A) and block A of the block copolymer (M_{bA}). Briefly, if $M_A < M_{bA}$, the homopolymer distributes throughout the A-rich domain. As M_A increases, A tends to concentrate in the center of the A-rich domain.[11] To the best of our knowledge, all of the related research has concentrated on characterizing the localization and spatial distribution of the homopolymer chains in the block domains. The conformation and orientation of the homopolymer chains confined to the block domains have not been studied due to the lack of suitable experimental techniques.

Characterization of polymer chain conformations requires a technique that has both high spatial resolution and the capability to distinguish the target polymer chain from the rest of the matrix. Fluorescence technique appears to be a very promising tool in the studies such as polymer conformation, morphology, and blend miscibility.[12,13] The merit of this technique is its high sensitivity associated with fluorescence (FL) detection. One needs only a trace amount of the FL chromophore to acquire information about a system, and the system itself will not be distorted significantly by the presence of the chromophore. Among fluorescence techniques, fluorescence microscopy is very powerful in detecting a single dye-labeled polymer chain in a nonfluorescent matrix. But because of the diffraction limit,[14] the highest resolution of a conventional fluorescence microscope can only reach about half of its excitation wavelength. This significantly limits its application in characterizing the conformation of a single polymer chain.

Scanning near-field optical microscopy (SNOM) is a novel technique that breaks the optical diffraction barrier. As a member of the family of scanning probe microscopies, SNOM is equipped with a quasi-point light source that has a diameter much smaller than the wavelength of the excitation light. By scanning the sample surface at a very close distance, SNOM can reach a resolution down to tens of nanometers.[15,16] The advantage of SNOM over other microscopy techniques arises not only from its ability to create high resolution, spectrally resolved optical images that allows one to study the objects within nanometer scale, but also from its nature of operating with light. As a complement to other techniques such as scanning tunneling microscopy, scanning electron microscopy, and atomic force microscopy, SNOM is extremely useful in nanoscience related to different optical properties, such as fluorescence, absorption, and polarization. In recent years, SNOM has been widely applied to many fields in polymer

* To whom correspondence should be addressed: e-mail aoki@photo.polym.kyoto-u.ac.jp; Tel +81-75-383-2613; Fax +81-75-383-2617.

10.1021/ma071350+ CCC: $37.00
Published on Web 09/25/2007

science such as studies on phase separation in polymer blend,[17] single-chain characterizations in polymer monolayers,[18] and investigations on the ordered structure of block copolymers.[19,20]

In this paper, we describe SNOM experiments on imaging single perylene-labeled poly(methyl mathacrylate) (PMMA-Pe) homopolymer chains embedded in lamellar domains formed by poly(styrene-*b*-methyl methacrylate) (PS−PMMA). We investigated the localization, shape, and orientation of single PMMA-Pe chains in the PMMA-rich domain of the block copolymer lamella. In order to observe polymer chain conformations and distinguish the chemically distinct domains of the block copolymer using SNOM, we chose PMMA-Pe and PS−PMMA with high molecular weights. The PS−PMMA has a lamellar spacing about 156 nm in bulk, and the two block domains can be easily distinguished by SNOM. Our results show that the PMMA-Pe chain has preferred orientation inside the PMMA block domain, and this preference depends on the location of the center of mass (CM) of the PMMA-Pe chain. However, the shape of a PMMA-Pe chain is almost independent of the location of the CM of the homopolymer in the block.

Experimental Section

Synthesis of Perylene-Labeled PMMA. Perylene-labeled poly(methyl methacrylate) (PMMA-Pe) was synthesized by radical copolymerization of methyl methacrylate (MMA) and 3-perylenyl methyl methacrylate at 55 °C for 24 h. 2,2′-Azobis(isobutyronitrile) (Wako) was used as the initiator. MMA (Wako) was purified by distillation under reduced pressure. 3-Perylenyl methacrylate monomer was synthesized by the reduction of 3-formylperylene following the Vilsmeiyer reaction of perylene.[21] The raw polymer obtained after polymerization was purified by fractional precipitation to obtain PMMA-Pe with narrow molecular weight distribution. The molecular weight of the synthesized PMMA-Pe was determined by gel permeation chromatography (D-7000G, Hitachi), with THF as the eluent and PMMA (American Polymer Standards Corp.) as the molecular weight standard. Signals were collected by tandem RI and UV (442 nm) detectors. The perylene fraction of the PMMA-Pe was determined from UV−vis absorption spectra by assuming that PMMA-Pe and perylene have the same extinction coefficient.

Sample Preparation. Symmetric PS−PMMA (molecular weight: 868 000 (PS)−857 000 (PMMA) g/mol; PDI: 1.3) was purchased from Polymer Source and used without further purification. We prepared four sets of PMMA-Pe/PS−PMMA mixtures (molar ratios of PMMA-Pe/PS−PMMA: 1.6×10^{-5}, 3.7×10^{-5}, 6.4×10^{-5}, and 9.0×10^{-5}), each of which was dissolved in chloroform (reagent grade, Wako) to form a 2 wt % solution. The polymer solutions were spread on clean glass plates. After drying, all of the films were annealed sequentially in chloroform vapor at room temperature (72 h) and in vacuum at 170 °C (24 h). In this way, we obtained a thick film (∼30 μm), with long-range ordered lamellar structure.

PMMA-Pe/PMMA thick film was prepared in a similar way, but without the solvent treatment. PMMA standard (Scientific Polymer Products Inc., M_n = 1 700 000 g/mol) was used as the matrix. We controlled the concentration of PMMA-Pe in PMMA at 0.0025 wt %. The polymer solution (1 wt % in toluene) was spread on glass plate and slowly dried at room temperature for 72 h. The dried thick film was then annealed in vacuum at 130 °C for 24 h and at 170 °C for 48 h.

All prepared thick films were removed from the glass substrates and sliced into ultrathin films (∼50 nm) by microtoming (Ultracut UTC, Leica microsystems). The sliced ultrathin films were then mounted on cover glass slips for the SNOM measurements.

SNOM Measurements. SNOM imaging was performed using a commercial α-SNOM (WITec) with a 441 nm laser (BCL-015-440, CrystaLaser) as the excitation source. A cantilever probe was used to scan the sample surface in contacting mode. The probe has a nanoaperture (∼60 nm) at the tip end, and the light passing through the aperture excites the perylene chromophores inside the polymer film. The signal light from the specimen was collected by a microscope objective (60×, 0.8 NA, Nikon) and split by a beam sampler. 4% of the collected signal was directed to an analog PMT (H5784, Hamamatsu Photonics) to obtain the transmission image, and the rest was detected by a photon counting PMT (H8631, Hamamatsu Photonics) after passing through a long-pass filter (LP02-442RS-25, Semrock) to acquire the fluorescence image. All images were recorded at a pixel size of 3.9 nm × 3.9 nm and a pixel dwell time of 3.9 ms. With our experimental setup, the surface topography (TP), fluorescence (FL), and transmission (TRANS) images can be simultaneously obtained from the scanning area.

Results and Discussion

Synthesis of PMMA-Pe and Sample Preparation. The synthesized PMMA-Pe after fractionation had the molecular weight (M_n) of 2 300 000 g/mol and polydispersity index 1.3. The GPC curve shows the PMMA-Pe free of unreacted dye monomers. It was found that 0.84% of the MMA monomer units in a PMMA chain had a perylene moiety attached to it, which is sufficient to give detectable fluorescence signal from a single polymer chain but not high enough to alter the physical properties of PMMA.

Treating block copolymer films with solvent vapor is very helpful to obtain long-range ordered structures.[22,23] We followed this method and treated the thick PS−PMMA films with chloroform vapor. The well-oriented lamellar structure inside the thick block copolymer film was significantly enhanced after the treatment. Although we were unable to obtain well-oriented lamellar pattern *throughout* the film, the size of the area with well-oriented lamellar structure in the thick film was large enough (∼10 μm × 10 μm) to obtain high-quality SNOM images. We also found that solvent vapor treatment had negligible effect on the lamellar spacing of PS−PMMA in bulk. The well-ordered lamellar structures inside the thick film have no preferred orientation relative to the film surface, resulting in extreme difficulties in slicing the thick film in the direction perpendicular to the lamellar alternating phases. We sliced the thick film in different directions relative to the film surface. All sliced thin films had thickness of about 50 nm. The acquired TRANS images showed no relationship between the slicing direction and the lamellar spacing. We take this result to mean that the sliced ultrathin films can be treated as quasi-two-dimensional planes, and the cutting direction has no effect on our SNOM results.

SNOM Imaging of a Single PMMA-Pe Chain. The objective of this research is to investigate the orientation and localization of single PMMA-Pe homopolymer chains in the PS−PMMA block copolymer lamella. We blended the PS−PMMA with different trace amounts of PMMA-Pe and imaged the ultrathin sliced films for each sample. The acquired FL images show that all fluorescent spots are homogeneously distributed throughout the sliced thin films. For each FL image (dimensions: 15 μm × 15 μm), we calculated the number density of the fluorescent spots by counting the number of fluorescent spots in the image. Figure 1 shows the observed number density of fluorescent spots at different PMMA-Pe/PS−PMMA ratios. The number density of fluorescent spots is in good agreement with the number density of PMMA-Pe chains in PS−PMMA matrix, based on the polymer molar ratio. This indicates that one fluorescent spot in the SNOM FL images corresponds to a single PMMA-Pe chain embedded in the block copolymer matrix.

Figure 2 shows a set of SNOM images obtained simultaneously from an area (1 μm × 1 μm) in a sliced PS−PMMA

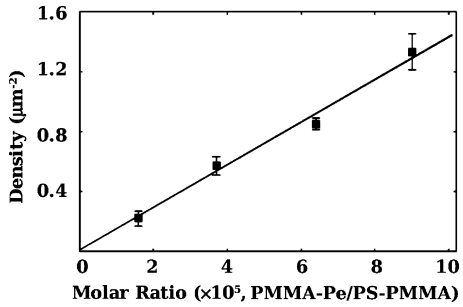

Figure 1. Number densities of fluorescent spots (solid squares with error bars) obtained from SNOM FL images at different PMMA-Pe/PS−PMMA ratios. For each ratio, we selected three different FL images (15 μm × 15 μm) and counted the number of fluorescent spots in each image. The density value with the error bar at each ratio is the averaged value with standard deviation. The solid line is the calculated number density of PMMA-Pe chains in the PS−PMMA matrix, based on the molar ratio of PMMA-Pe to PS−PMMA.

ultrathin film doped with PMMA-Pe. The TP image (a) shows no surface feature and can hardly provide any useful information about the morphology or polymer chain conformation. The TRANS image (b) clearly shows the alternative local contrast between the two block domains of the PS−PMMA. This contrast may originate from the different refractive indices of PS (1.59) and PMMA (1.49).[24] The bright areas correspond to the PMMA domains and the dark parts are the areas occupied by the PS blocks (see Supporting Information for the identification of the two domains). The bright spot in the FL image (c) corresponds to the single PMMA-Pe chain embedded in the block copolymer lamella. (d) is a pseudo-colored superimposed image of (b) and (c), which indicates the location and orientation of the homopolymer chain in the PMMA-rich domain layer of the PS−PMMA lamella.

Analyses of SNOM Images. The FL image of the PS−PMMA/PMMA-Pe mixture provides rich information about the location and orientation of the PMMA-Pe chain, while the TRANS image contains information about the lamellar structure of the block copolymer. By analyzing the FL and TRANS images, we were able to determine the relative position and orientation of the PMMA-Pe chain inside the PMMA-rich domain layer of the PS−PMMA block copolymer lamella. A typical procedure of the image analysis may be described as follows:

1. Characterization of the Conformation, Orientation, and Center of Mass of a Single PMMA-Pe Chain. We followed a standard procedure to analyze the chain conformations of the PMMA-Pe chains shown in the acquired FL images.[25,26] Briefly, as shown in Figure 3, we select an area including the bright spot in the FL image and read the fluorescence intensity at every pixel throughout this area. The normalized second moments of the fluorescence intensity distribution (M) in two dimensions are expressed as

$$M_{xx} = \frac{1}{I_0}\sum_{i,j} I_{ij}(x_{ij} - x_{CM})^2; \quad M_{yy} = \frac{1}{I_0}\sum_{i,j} I_{ij}(y_{ij} - y_{CM})^2$$

$$M_{xy} = M_{yx} = \frac{1}{I_0}\sum_{i,j} I_{ij}(x_{ij} - x_{CM})(y_{ij} - y_{CM}) \qquad (1)$$

where I_0 is the sum of the intensity of the selected area and (x_{ij}, y_{ij}) is the Cartesian coordinate of the pixel (i, j) in the image. M is a tensor and stands for the anisotropic intensity distribution of the investigated fluorescent spot (corresponds to a PMMA-Pe coil). The coordinate of the intensity-weighted center of mass (CM) of the PMMA-Pe chain is

$$x_{CM} = \frac{1}{I_0}\sum_{i,j} I_{ij}x_{ij}; \quad y_{CM} = \frac{1}{I_0}\sum_{i,j} I_{ij}y_{ij} \qquad (2)$$

The tensor **M** is a measure of the size and shape of the PMMA-Pe polymer chain. In this way, the investigated polymer chain spot can be represented as an ellipse with long and short principal axes. The eigenvalues of the long (λ_l) and the short (λ_s) principal axes are given by

$$\lambda_{l,s} = \frac{\mathrm{tr}(\mathbf{M}) \pm \sqrt{\mathrm{tr}(\mathbf{M})^2 - 4\,\det(\mathbf{M})}}{2}; \quad \mathbf{M} = \begin{pmatrix} M_{xx} & M_{xy} \\ M_{yx} & M_{yy} \end{pmatrix} \qquad (3)$$

where tr(**M**) and det(**M**) are the trace and the determinant of **M**. The trace of **M** defines the radius of gyration, $R_g^2 = \mathrm{tr}(\mathbf{M})$. The orientation of the PMMA-Pe chain is defined as the orientational angle (θ) of the long principal axis relative to the positive X-axis

$$\theta = \arctan\left(\frac{\lambda_l - M_{xx}}{M_{xy}}\right) \qquad (4)$$

2. Determination of Lamellar Spacing and Lamellar Orientation. The periodical spacing and the orientation of the PS−PMMA lamella were determined from the fast Fourier transform (FFT) of the TRANS images, as shown in Figure 4.[27] Figure 4a is the duplicated TRANS image of Figure 2b, which shows the lamellar structure formed by the PS−PMMA block copolymer. FFT (inset of Figure 4a) of the TRANS image shows an ordered pattern of the lamellar structure in the reciprocal space. We drew a line that passes through the pattern and counted the intensity along the line. The direction of the line indicates the orientation of the lamellar structure (lamellar normal). We defined the angle between the orientation of the PMMA-Pe chain and the lamellar normal as the relative orientational angle of the PMMA-Pe chain embedded in the PS−PMMA lamella.[28] The lamellar spacing of PS−PMMA is 156 ± 6 nm, calculated from the distance between the characteristic peaks in the intensity distribution profile, as shown in Figure 4b.

3. Determination of the CM Location of a PMMA-Pe Chain in the Lamella. We located the CM of the PMMA-Pe chain, calculated from Figure 3 and eq 2, in the TRANS image. In Figure 5a, the CM of PMMA-Pe is indicated as a white circle in the TRANS image. The black solid line passes through the CM and has the same orientation as the block copolymer lamellar normal. We tracked the transmission intensity in the TRANS image across the PMMA-rich domain along this solid line. The transmission intensity distribution, shown as the open circles in Figure 5b, was then fitted to a modified Helfand−Tagami hyperbolic function[29]

$$I(x) = a + b\left\{\tanh\frac{2[(x-c)+d]}{\delta} - \tanh\frac{2[(x-c)-d]}{\delta}\right\} \qquad (5)$$

In eq 5, $I(x)$ is the fitted transmission intensity distribution across the PMMA-rich domain, along the solid line shown in Figure 5a. x is the coordinate along the solid line. a, b, c, d, and δ are the floating parameters used in the fitting. Among those parameters, c refers to the distance between the CM and the center of the PMMA-rich domain layer in the direction of the

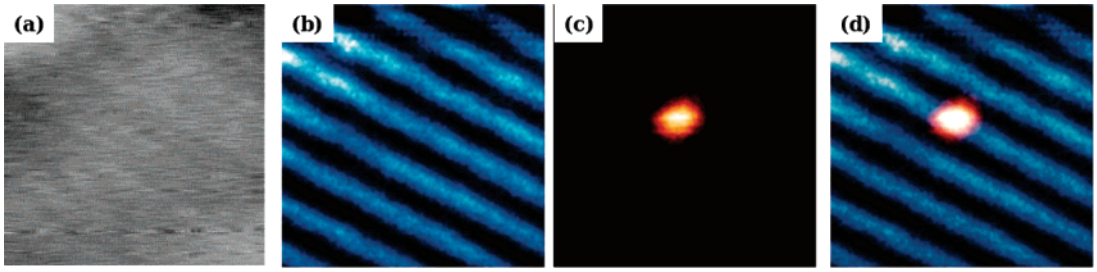

Figure 2. Topography (a), transmission (b), fluorescence (c), and superimposed (b and c) images of a scanning area in a PS−PMMA/PMMA-Pe thin film. The dimension of all images is 1 μm × 1 μm. The lamellar pattern shown in (b) corresponds to the lamellar morphology formed by PS−PMMA. The blue and dark parts in the image correspond to PMMA and PS, respectively. The bright spot in (c) corresponds to a single PMMA-Pe chain embedded in the PS−PMMA matrix. The pseudo-colored superimposed image (d) shows the location and orientation of the PMMA-Pe homopolymer chain in the PS−PMMA lamella.

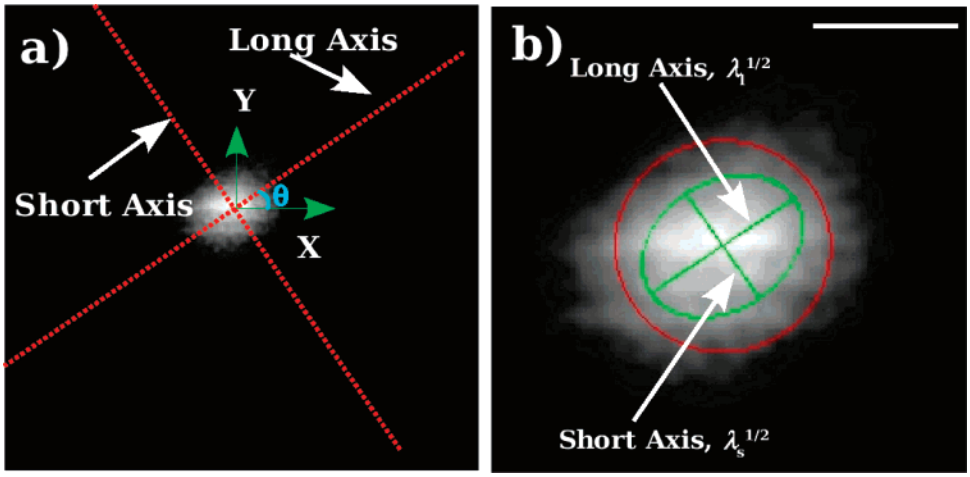

Figure 3. Determination of the orientation and the center of mass of a PMMA-Pe chain. (a) Duplicated FL image of Figure 2c (dimension: 1 μm × 1 μm). The bright white spot corresponds to a single PMMA-Pe chain. The chain orientation, indicated as the long axis, is calculated on the basis of the method described in the text. The short axis is perpendicular to the chain orientation. The center of mass of the PMMA-Pe chain is located at the intersection of the two axes. The orientational angle (θ) of the polymer chain is indicated in the figure. (b) Enlarged image of the PMMA-Pe chain shown in (a). The radius of the red circle is the calculated R_g of the PMMA-Pe chain. The green ellipse is drawn with the square roots of the two eigenvalues (λ_l and λ_s) as the long and short axes. The long axis defines the orientation of the PMMA-Pe chain. The scale bar in (b) is 100 nm.

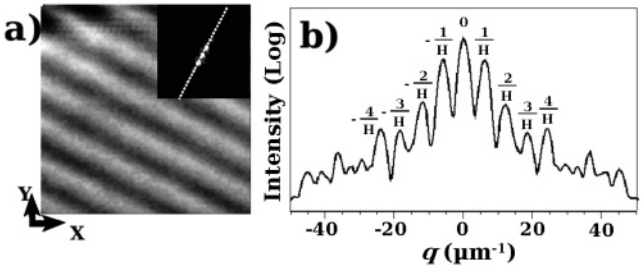

Figure 4. Determination of the orientation and the spacing of a sample lamellar structure formed by PS−PMMA. (a) TRANS image and its fast Fourier transform (FFT) image (inset). The white dotted line passes through the pattern in the FFT image and shows the orientation of the lamellar structure (lamellar normal). (b) Intensity distribution along the dotted line shown in the inset of (a). The ordered peaks are indicated in the figure. *H* is the lamellar spacing.

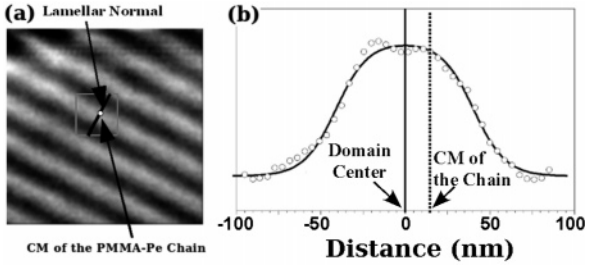

Figure 5. Location of the center of mass (CM) of a PMMA-Pe homopolymer chain in the PS−PMMA lamella (a) and cross-section profile in the normal direction to the lamella (b). (a) TRANS image duplicated from Figure 2b. The CM of the Pe-PMMA is shown as the white spot. The solid line is the line path used to calculate the cross-section profile of the transmission intensity. It passes through the CM of the PMMA-Pe and has the same orientation as the PS−PMMA lamellar normal. (b) Cross-section distribution (open circles) of the transmission intensity recovered from (a) along the solid line. The solid curve in (b) is the fitted intensity profile (eq 5). We set the origin of the distance coordinate to the center of the PMMA-rich layer. The coordinate of the dashed line represents the distance between the CM of the PMMA-Pe and the center of the PMMA-rich domain.

lamellar normal. δ is the width of the interface between the PS and PMMA domains. We defined the full width at half-maximum (FWHM) of the fitted profile as the width of the PMMA-rich domain.

Using our methodology of the SNOM image analysis, we analyzed 100 PMMA-Pe chains located at different areas in the PS−PMMA lamellae. We calculated the orientational angle of each PMMA-Pe chain relative to the lamellar normal and the relative position of the PMMA-Pe chain located in the PMMA-rich domain of the copolymer matrix. All information was compiled to construct the relationship between the chain orientation and the location of PMMA-Pe in the PS− PMMA lamella.

Localization of PMMA-Pe Chains in the PS−PMMA Lamella. Russell and co-workers investigated the localization of PMMA homopolymers in PS−PMMA block copolymer lamellae, using specular neutron reflectivity.[8,9] According to their results, the localization of PMMA homopolymer in the PS−

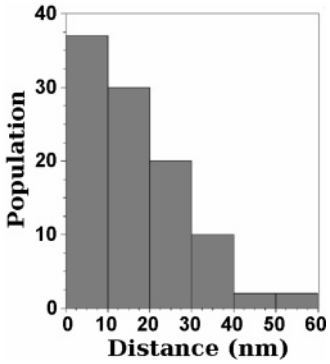

Figure 6. Histogram of the localization of PMMA-Pe in the PMMA-rich domain of the PS−PMMA block copolymer lamella. The population of PMMA-Pe chains is plotted against the distance between the CM of a PMMA-Pe chain and the center of the PMMA-rich domain (parameter c in eq 5). The average size of half of the PMMA-rich domain is 41 ± 5 nm (half of the fwhm in eq 5).

PMMA lamella depends on the molecular weights of the PMMA (M_{h-PMMA}) and the PMMA block of the PS−PMMA (M_{b-PMMA}):

If M_{h-PMMA} is small compared to M_{b-PMMA}, the PMMA homopolymer tends to distribute throughout the PMMA domain homogeneously; if M_{h-PMMA} is comparable to M_{b-PMMA}, the homopolymer tends to distribute in the domain with the highest concentration at the center; if M_{h-PMMA} is much larger than M_{b-PMMA}, the PMMA chains segregate from the block domain and form relatively small domains distributed throughout the film. In our experiments, we are interested in characterizing a single polymer chain in a copolymer matrix. The extremely low concentration of PMMA-Pe in the matrix is unfavorable for the aggregation of PMMA-Pe. As a consequence, individual homopolymer chains will be isolated in the copolymer matrix. The location and conformation of the single polymer chain depend on the local enthalpic interactions between the homopolymer chain and the surrounding block copolymer chains.

In Figure 6, we show a histogram of the localization of the 100 PMMA-Pe chains in PS−PMMA. In this figure, the population of PMMA-Pe chains is plotted against the distance between the CM of the PMMA-Pe chain and the center of the PMMA-rich domain layer. The average size of half of a PMMA domain was found to be 41 ± 5 nm. It is easily seen that the PMMA-Pe chains are neither homogeneously distributed in the PMMA-rich domain nor all confined to the center of the block domain layer. The FL images show that segments of the PMMA-Pe chains distribute throughout the PMMA-rich domain. We found that more than 90% of the CMs of PMMA-Pe chains were located in the PMMA-rich domain, and the center of the PMMA-rich domain had the highest CM population. Few PMMA-Pe chains protrude from the PMMA-rich domain and entangle with the PS block chains. The embedded PMMA-Pe homopolymers have an average R_g of 88 ± 13 nm. This value is smaller than the R_g of the PMMA-Pe in the PMMA matrix (117 ± 13 nm).[30] The synthesized PMMA-Pe has a molecular weight (2 300 000 g/mol) 3 times larger than that of the PMMA block (857 000 g/mol) of the PS−PMMA sample. The difference of the two R_g's clearly shows the confinement effect of the block copolymer lamella on the conformation of the embedded PMMA-Pe homopolymer.[31] Segments of the individual homopolymer chains crowd into the PMMA-rich domain layers due to the repulsive interaction between PMMA-Pe and PS. The FL images also show that the compression of the PMMA-Pe chain is not homogeneous, resulting in a certain orientation along the calculated long principal axis. The average square roots of the two eigenvalues of the PMMA-Pe chains were found to be 67 ± 10 and 56 ± 8 nm in the direction parallel with and perpendicular to the chain orientation, respectively. The difference is small and independent of the CM location of the PMMA-Pe chains, indicating that the restricted PMMA-rich domain in a PS−PMMA lamella only has a moderate effect on the anisotropic deformation of the embedded PMMA-Pe chains.

Relative Orientation of PMMA-Pe Chain in PS−PMMA Lamella. Although the deformation of the homopolymer chains inside the block domain is less than what we expected, the orientation of an embedded PMMA-Pe chain can still be accurately determined using the method described in the section of image analysis. We constructed a relationship between the orientation and location of homopolymer chains embedded in the PMMA-rich domains of the block copolymer lamella. As shown in Figure 7a, for each PMMA-Pe chain, the angle between the chain orientation and the lamellar normal was plotted against the relative CM position of the homopolymer chain in the block domain. We found a weak tendency that the homopolymer chains oriented themselves depending on their locations in the PMMA-rich domain layer. When the CM of PMMA-Pe is at the center of the PMMA-rich domain layer, the homopolymer prefers an orientation parallel to the lamella phase; i.e., the orientation has an angle of 90° from the lamellar normal. When the PMMA-Pe chain is situated close to the interface, its orientation tends to be perpendicular to the lamella phase. In Figure 7a, we also show superimposed (FL and TRANS) images of three PMMA-Pe chains located at different positions in the PMMA-rich domain. From the three images, one can easily see the tendency of the orientational change with distance between the CM of PMMA-Pe and the center of the PMMA-rich layer.

Figure 7b shows the shape parameter, defined as the square root of the ratio between the two eigenvalues of the long (λ_l) and the short (λ_s) principal axes, of a PMMA-Pe homopolymer chain relative to its location in the block copolymer lamellae. Although we found the PMMA-Pe chain had weak preferred orientation depending on its location in the block copolymer lamella, the shape of a homopolymer chain seems to have no relationship with its CM location. Moreover, the blurring effect, caused by the finite dimension of the aperture on the SNOM probe, always exists in the fluorescence imaging. This blurring effect makes the fluorescent object more roundlike than its real shape. As a consequence, it is difficult to compare the shape determined from the FL image to the real shape of the PMMA-Pe homopolymer chain. Here we only showed the determined shape parameters of the PMMA-Pe chains, and were reluctant to draw further conclusions about the shape of the homopolymer chains.

We show a sketch of the position dependence of the PMMA-Pe chain orientation in the PS−PMMA block copolymer lamella in Figure 8. It is well-known that the system free energy of a neat, phase-separated block copolymer system can be split into an interfacial and a stretching contribution.[1] The interfacial free energy includes the contact enthalpy between the blocks and the confinement entropy originating from the selective location of the block chains in the ordered structure. The stretching energy is caused by the extension of the block chain, which tends to compensate for the unfavorable contact with the different block type. The chain stretching effect causes preferred orientation of the block chains perpendicularly to the lamellar phase.[5] When an ordered structure is formed, all energetic contributions balance each other to minimize the overall free energy of the system. If the PMMA-Pe chains sparsely locate

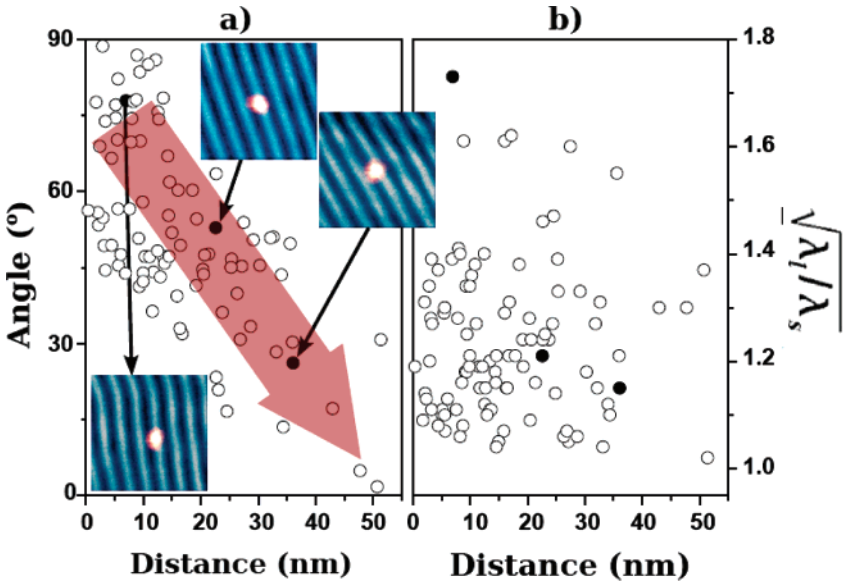

Figure 7. (a) Plot of chain orientation of PMMA-Pe against the CM location in the PMMA-rich domains of PS−PMMA lamellae. *Y*-axis shows the relative angle between the chain orientation and the lamellar normal. *X*-axis shows the distance between the CM of PMMA-Pe and the center of the corresponding PMMA-rich domain layer. Superimposed images (FL and TRANS) of three PMMA-Pe chains located in different areas in the PS−PMMA block copolymer lamellae are also shown in the figure. The corresponding CM positions of the three PMMA-Pe chains in the figure are indicated as the solid points. The transparent broad red arrow serves as a guide for the eye. The bright spot in each of the superimposed images corresponds to the single PMMA-Pe chain. (b) Plot of the shape parameter (defined as the square root of the ratio between the two eigenvalues of the long (λ_l) and the short (λ_s) principal axes) of a PMMA-Pe homopolymer chain against its CM location in the PS−PMMA block copolymer lamellae. The *X*-axis has the same meaning as that in (a). The three PMMA-Pe chains shown in the superimposed images are also indicated as solid points.

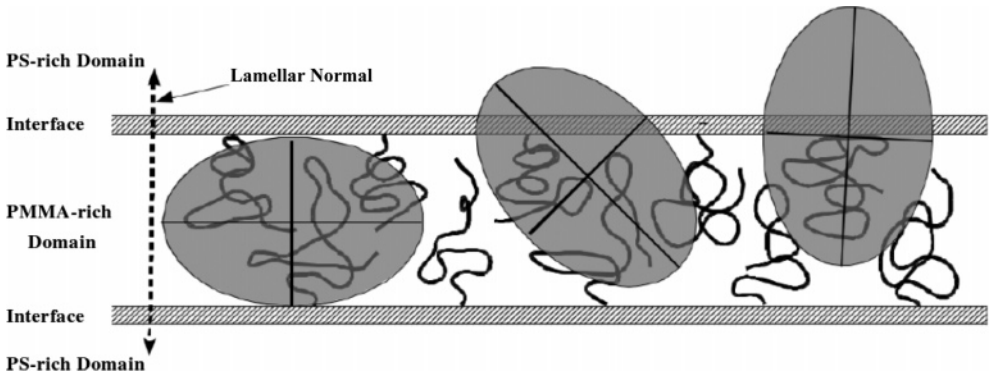

Figure 8. Sketch showing the relationship between the orientation and location of PMMA-Pe chains inside a PMMA-rich domain layer. The black coils represent the PMMA block chains. The elliptical shadows stand for the PMMA-Pe chains with specific conformation and orientation inside the block domain (see the image analysis section). The longer black line in each shadow indicates the orientation of the specific PMMA-Pe chain. The CM of the PMMA-Pe chain is located at the intersection of the two black lines in each shadow.

in a matrix of PS−PMMA lamellae, the individual chains are confined to the PMMA-rich domain due to the repulsive interaction between the PS block and the PMMA-Pe chain. This confinement results in entropy loss of the system, and as an energetic compensation, the PMMA-Pe chain will have preferred location and orientation in the PMMA-rich domain. Since the investigated PMMA-Pe has a molecular weight 3 times larger than that of the PMMA block, to minimize the system energy, the PMMA-Pe chains tend to locate at the center of the PMMA-rich domain. Meanwhile, the PMMA-Pe chains are compressed and, most likely, anisotropically deformed in the direction parallel with the lamella phase due to the large molecular weight of the homopolymer. In a neat block copolymer lamella, the simulation results showed that the segments close to the end of the block chain had more rotational freedom than those close to the block junction.[32] If the homopolymer chain is at the center of the domain layer, it is in an environment that allows the homopolymer chain to rotate more freely upon annealing. The homopolymer chain can easily rotate and rearrange itself to minimize the local free energy in its neighborhood. The homopolymer chain will, therefore, have preferred orientation parallel to the lamella phase.

Although most of the PMMA-Pe chains locate at the center of the PMMA-rich domain, our results show that, for some homopolymer chains, part of the chain segments are in areas close to the block interface, or even in the PS domain, due to fluctuations. When most of the segments of the homopolymer chain are localized close to the block interface, the rotational movement of the homopolymer chain is much retarded by block chains (lack of rotational freedom). Segments can rearrange alongside the block chains only during annealing. The block chains have preferred orientations perpendicular to the lamellar phase due to the chain stretching effect, and the homopolymer chains close to interfacial area will also have preferred orientations perpendicular to the lamella.

Possible Distortion of the FL Image in the SNOM Measurements.[33] The possible distortion of the FL images obtained from our SNOM experiments may originate either from

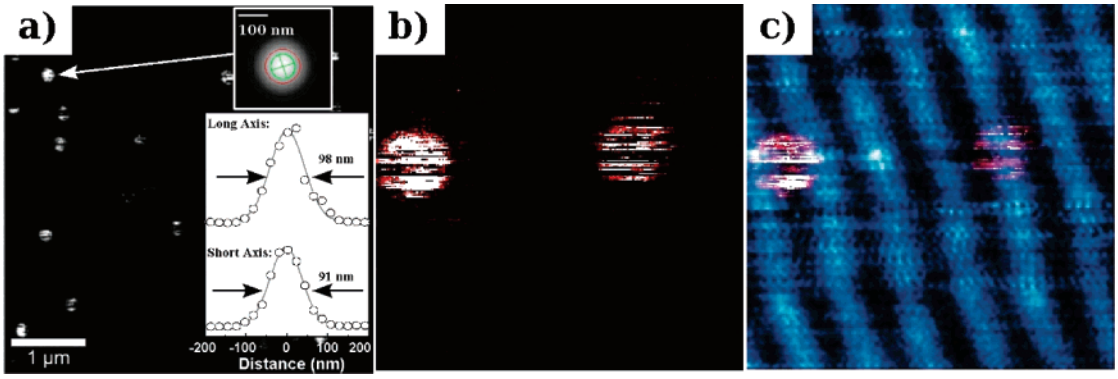

Figure 9. (a). Fluorescence (FL) image of QDs on a microtomed block copolymer film with lamellar structure. The upper inset shows the enlarged image of an investigated QD, indicated by the arrow. The lower inset shows the intensity distribution along the long and the short axes. The two values of FWHM are indicated in the inset. (b). FL image of two QDs located on a microtomed PS−PMMA block copolymer film. We adjusted the intensity scale to show both QDs clearly. (c) FL image shown in (a) superimposed on the TRANS image of the same SNOM scanning area. The dimension of images (b) and (c) is 1 μm × 1 μm.

the finite dimension the aperture on the SNOM probe or from the change of the refractive index in the alternating PS and PMMA domains. The distortion of FL image can be tested by imaging an infinitely small single fluorescent object. The nanocrystal of semiconductor, quantum dot (QD), is a good candidate due to its bright fluorescence and infinitely small size compared to the SNOM aperture. The fluorescence image of a QD directly indicates the point spread function of the apparatus.

We spin-coated a thin layer (∼20 nm) of poly(vinyl alcohol) (PVA, Wako, degree of polymerization ∼ 2000) on the microtomed PS−PMMA block copolymer thin film. The PVA film was doped by QDs (Qdot 655 ITK, Invitrogen) at an ultradiluted concentration. We imaged individual QDs located on the block copolymer film with lamellar structure. Figure 9a is a FL image that shows several QDs on a block copolymer film. Since the irregular blinking of QD makes the image analysis difficult, we only tried to analyze one of the QDs using our methodology described previously. Results show that the QD has a near-round shape with an averaged value of FWHM about 95 nm. Figure 9b shows a high-resolution FL image with two QDs on the PS−PMMA block copolymer lamella. The near-round shape of the fluorescent spots in the FL image indicates that the effect of the image distortion in our SNOM experiment is not obvious. Furthermore, as shown in Figure 9c, the intensity distributions of the QDs are not related to the positions of QDs on the PS−PMMA lamella, which is good evidence that the change of the refractive index across the different block domains in the block copolymer film has negligible effect on the FL imaging of QD.

Conclusions

In this paper, we report studies on the localization and orientation of single PMMA-Pe homopolymer chains in a PS−PMMA block copolymer lamella. Our results show that most of the dispersed PMMA-Pe chains are localized in the PMMA-rich layers. The PMMA-Pe chains are deformed due to the confinement of the block domains of the block copolymer. But the extent of the deformation is neither significant nor dependent on the chain location. We, for the first time, report the orientational preference of the homopolymer chain in the block domain. The orientation of the homopolymer chain has a weak dependency on the location of the homopolymer inside the block domain. When the homopolymer is situated at the center of the domain layer, it has an orientation parallel to the lamellar phase. With the increase of the distance between the CM of homopolymer chain and the center of the domain layer, the homopolymer chain tends to orient itself perpendicularly to the interface. We consider this a result of the rotational freedom of the homopolymer in the block domain of the block copolymer lamella.

Acknowledgment. This work is supported by the Grant-in-Aid from the Japan Society for the Promotion of Science (JSPS) and from the Ministry of Education, Culture, Sports, Science and Technology (MEXT), Japan. This work is partly supported by Innovative Techno-Hub for Integrated Medical Bio-imaging Project of the Special Coordination Funds for Promoting Science and Technology from MEXT. J. Yang acknowledges a post-doctoral fellowship from JSPS. The authors also thank Dr. John G. Spiro (University of Toronto, Canada) for his kind help in the revision of this manuscript.

Supporting Information Available: Descriptions of experiments on distinguishing PS and PMMA domains in the PS−PMMA lamella. This material is available free of charge via the Internet at http://pubs.acs.org.

References and Notes

(1) Bates, F. S.; Fredrickson, G. H. *Annu. Rev. Phys. Chem.* **1990**, *41*, 525.
(2) Hamley, I. W. *The Physics of Block Copolymers*; Oxford University Press: New York, 1998.
(3) Shull, K. R.; Winey, K. I. *Macromolecules* **1992**, *25*, 2637.
(4) Vavasour, J. D.; Whitemore, M. D. *Macromolecules* **2001**, *34*, 3471.
(5) Matsushita, Y.; Mori, K.; Saguchi, R.; Nakao, Y.; Noda, I.; Nagasawa, M. *Macromolecules* **1990**, *23*, 4313. Hasegawa, H.; Hashimoto, T.; Kawai, H.; Lodge, T. P.; Amis, E. J.; Glinka, C. J.; Han, C. C. *Macromolecules* **1985**, *18*, 67. Matsushita, Y.; Mori, K.; Mogi, Y.; Saguchi, R.; Noda, I.; Nagasawa, M.; Chang, T.; Glinka, C. J.; Han, C. C. *Macromolecules* **1990**, *23*, 4317. Koizumi, S.; Hasegawa, H.; Hashimoto, T. *Macromolecules* **1994**, *27*, 7893.
(6) Winey, K. I.; Thomas, E. L.; Fetters, L. J. *Macromolecules* **1992**, *25*, 2645.
(7) Orso, K. A.; Green, P. F. *Macromolecules* **1999**, *32*, 1087.
(8) Mayes, A. M.; Russell, T. P.; Satija, S. K.; Majkrzak, C. F. *Macromolecules* **1992**, *25*, 6523.
(9) Shull, K. R.; Mayes, A. M.; Russell, T. P. *Macromolecules* **1993**, *26*, 3929.
(10) Rharbi, Y.; Zhang. J.; Spiro, J. G.; Chen, L.; Winnik, M. A.; Vavasour, J. D.; Whitmore, M. D.; Jérôme, R. *Macromolecules*, **2003**, *36*, 1241.
(11) Koizumi, S.; Hasegawa, H.; Hashimoto, T. *Macromolecules* **1994**, *27*, 6532.
(12) Winnik, M. A., Ed. *Photophysical and Photochemical Tools in Polymer Science;* Reidel: Dordrecht, 1985.
(13) Tanaka, T., Ed. *Experimental Methods in Polymer Science*; Academic: San Diego, 2000; Chapter 3.
(14) Abbe, E. *Arch. Mikrosk. Anat.* **1873**, *9*, 413.
(15) Betzig, E.; Trautman, J. K. *Science* **1992**, *257*, 189.
(16) Dunn, R. *Chem. Rev.* **1999**, *99*, 2891.

(17) Aoki, H.; Kunai, Y.; Ito, S.; Yamada, H.; Matsushige, K. *Appl. Surf. Sci.* **2002**, *188*, 534.
(18) Aoki, H.; Anryu, M.; Ito, S. *Polymer* **2005**, *46*, 5896.
(19) Fasolka, M. J.; Goldner, L. S.; Hwang, J.; Urbas, A. M.; DeRege, P.; Swager, T.; Thomas, E. L. *Phys. Rev. Lett.* **2003**, *90*, 016107.
(20) Raschke, M. B.; Molina, L.; Elsaesser, T.; Kim, D. H.; Knoll, W.; Hinrichs, K. *ChemPhysChem* **2005**, *6*, 2197.
(21) Aoki, H.; Ito, S. *J. Phys. Chem. B* **2001**, *105*, 4558.
(22) Kim, S. H.; Misner, M. J.; Xu, T.; Kimura, M.; Russell, T. P. *Adv. Mater.* **2004**, *16*, 226.
(23) Xuan, Y.; Peng, J.; Cui, L.; Wang, H.; Li, B.; Han, Y. *Macromolecules* **2004**, *37*, 7301.
(24) Brandrup, J., Immergut, E. H., Eds. *Polymer Handbook*, 3rd ed.; John Wiley & Sons: New York, 1989.
(25) Maier, B.; Rädler, J. O. *Rhys. Rev. Lett.* **1999**, *82*, 1911.
(26) Maier, B.; Rädler, J. O. *Macromolecules* **2001**, *34*, 5723.
(27) The FFT on the TRANS images was performed via Gwyddion, a free SPM data analysis framework developed under the terms of the GNU General Public License.
(28) The angle between chain orientation and the orientation of the lamellar structure is in the 0−90° range. For a calculated value (α) larger than 90°, we use 180° − α as the angle.
(29) Helfand, E.; Tagami, Y. *J. Chem. Phys.* **1972**, *56*, 3592. Helfand, E.; Wasserman, Z. R. *Macromolecules* **1976**, *9*, 879.
(30) We followed the same method to calculate the FWHM of PMMA-Pe in the PMMA matrix. FL images show that the PMMA-Pe has no preferred orientation in the PMMA matrix. We analyzed 40 fluorescent spots, each of which corresponds to single PMMA-Pe chains, and averaged all R_g values.
(31) The values of R_g obtained from the analysis of the FL image contain the blurring effect of fluorescence due to the finite dimension of the aperture on the SNOM probe. As a consequence, the determined values of R_g are larger than those measured by the small-angle neutron scattering (SANS).
(32) Yang, J.; Winnik, M. A.; Pakula, T. *Macromol. Theory Simul.* **2005**, *14*, 9.
(33) After we submitted this manuscript to *Macromolecules*, the reviewers raised questions about the possible distortion in the FL images in our SNOM experiments. We believe this issue is worth a brief discussion in this paper. Therefore, we added the discussion of the possible image distortion as an independent section at the end of this paper.

MA071350+